WALAILAK JOURNAL
http://wjst.wu.ac.th Engineering and Physical Sciences

A Comparison of Landslide Susceptibility Maps Produced by Weighted Linear Combination and Analytical Hierarchy Process Methods: A Case Study at Khao Phanom Bencha Watershed in Krabi Province

Thidapath ANUCHARN* and Songkot DASANANDA

School of Remote Sensing, Institute of Science, Suranaree University of Technology, Nakhon Ratchasima 30000, Thailand

(*Corresponding author's e-mail: thidapath.a@gmail.com)

Received: 11 February 2016, Revised: 12 July 2016, Accepted: 29 August 2016

Abstract

This study compared the abilities of the Weighted Linear Combination (WLC) and Analytical Hierarchy Process (AHP) methods in producing credible landslide susceptibility maps for the study area at Khao Phanom Bencha Watershed in Krabi Province, southern Thailand. A reference landslide inventory was established from identified landslide events appearing on 4 sources of high-resolution satellite imagery (THEOS, EO-1, Google Earth, and Bing Map). Ten crucial contributing factors were incorporated in the susceptibility analysis in both methods, i.e., elevation, slope gradient, slope aspect, slope curvature, Topographic Wetness Index (TWI), distance from drainage, distance from lineament, lithology, soil texture, and land use/land cover (LULC). All yielded susceptibility maps were assessed for their respective accuracies in predicting the referred landslide incidences (290 samples in total), based on 2 well-known methods: the Area-Under-Curve (AUC) and the Receiver Operating Characteristic (ROC) analysis. Average accuracies of the maps achieved by the WLC and AHP methods were found to be significantly high, at 85.81 and 82.42 %, respectively. These maps are useful for the preparation of effective strategic planning for the prevention and mitigation of landslide hazards in the area by responsible agencies and local authorities.

Keywords: Landslide susceptibility map, Weighted Linear Combination (WLC), Analytical Hierarchy Process (AHP), Area-Under-Curve (AUC), Receiver Operating Characteristic (ROC)

Introduction

Landslides are well-known natural phenomena involving a mass movement of soil (in the forms of earth or debris) or rock downward along a slope under gravitational influence [1,2]. At present, landslides are regarded as one of the most destructive of hazards, which induces a substantial loss of life and vast damage to property and the natural environment worldwide [3-5]. Therefore, prior knowledge of the areas prone to destructive landslides is highly essential for most countries, especially those in the tropics or in the earthquake dominated zone, to help with preparing proper strategies for the prevention or mitigation of the potential landslide risk. Conventionally, a detailed map illustrating the distribution of these landslide-prone areas is called a landslide susceptibility map.

In principle, there are 2 broad groups of landslide susceptibility evaluating methods; the qualitative (or heuristic) type, and the quantitative type. For the qualitative approach, the final decision on landslide potential over an area is determined based mainly on collective expert opinions (on the nature of landslide characteristics experienced within an area). This concept was widely used as a basic methodology for the construction of initial landslide susceptibility zoning by landslide researchers for a long time. However, in recent decades, more complicated methods of the quantitative type, which make decisions on this issue

based on information on past landslide events that have taken place in the area, were introduced to build more realistic susceptibility maps for an area; these methods include the frequency ratio (FR) or Multiple Logistic Regression (MLR) methods, e.g., in [6-9].

Attention paid to the identification of landslide prone areas (or susceptibility analysis) and the assessment of the potential impacts on humans and the environment (risk analysis) has risen dramatically in recent decades, due to mounting public concern on these issues. As validity of a gained landslide susceptibility map depends principally on the used methods and their input data, comparative studies to evaluate the efficiency of several recommended methods in the preparation of landslide susceptibility maps for an area of interest has been reported more often in recent years, such as [5,10-14]. The main objectives of these studies were to identify the capability of the tested methods in generating a high-accuracy landslide susceptibility map for the preferred area, from which the most effective procedure can then be applied in subsequent hazard and risk analysis.

For this work, the capability of 2 popular qualitative methods; the Weighted Linear Combination (WLC) and Analytical Hierarchy Process (AHP), was evaluated and compared for the study area of Khao Phanom Bencha Watershed in Krabi Province, southern Thailand. This place was chosen due primarily to its status as one of the landslide hotspots in Thailand, where devastating landslide incidences were reported several times in recent decades. The referred area is located on the Andaman Coast of southern Thailand, covering land of about 987.53 km^2 and dominated by mountainous topography (**Figure 1**). The watershed has a central mountain network that aligns along the north-south direction, approximately, as its outstanding landmark. Frequent landslide activities occur as a result of the rough mountainous landscape and a fairly high amount of annual rainfall [15]. However, rapid changes in land use patterns in the area, due to continuous conversion of the forest lands into several kinds of economic agricultural plantations (e.g., para rubber and oil palm) and communities into the known landslide-prone locations, have recently become a cause for high public concern. This is because forest clearance for expansive plantations of the shallow-rooted crops, orchards, or trees, might enable more massive landslide incidence, with higher losses of human lives or higher amount of gross damages to important infrastructures and the natural environment [16,17].

Figure 1 Location map of the study area, Khao Phanom Bencha Watershed in Krabi Province.

Materials and methods

Materials

The required input data were acquired from responsible agencies and from other relevant resources (as detailed in **Table 1**) and then restructured to have the proper format for further use (in the form of a GIS-based dataset). Ten typical causative factors of landslide activity in tropical zones were included in the construction of the preferred susceptibility map: elevation, slope gradient, slope aspect, slope curvature, Topographic Wetness Index (TWI), distance from drainage, distance from lineament, lithology, soil texture, and Land Use/Land Cover (LULC) (**Figures 2(a) - (j)**). These factors can be grouped into 3 broad categories: geological, topographical and environmental types.

Table 1 List of necessary input data and their respective sources.

Classification		GIS	Scale or	Original	Note
Data category	**Details**	**data type**	**resolution**	**sources**	
Land use/Land cover	LULC-2009	Polygon	1:25,000	LDD	**Figure 2(j)**
Topography	Elevation	Point/Line	1:50,000	RTSD	**Figure 2(a)**
	Slope gradient				**Figure 2(b)**
	Slope aspect				**Figure 2(c)**
	Slope curvature				**Figure 2(d)**
Landform	TWI				**Figure 2(e)**
Stream	Stream network				**Figure 2(f)**
Geology	Lithology	Polygon	1:250,000	DMR	**Figure 2(h)**
	Lineament	Line	1:250,000	DMR	**Figure 2(g)**
Soil	Soil texture	Polygon	1:100,000	LDD	**Figure 2(i)**

Note: DMR ≡ Department of Mineral Resources; LDD ≡ Land Development Department; RTSD ≡ Royal Thai Survey Department.

Methods

Construction of landslide inventory map

The landslide inventory map was formulated based on accumulated data of past landslide occurrences within the area, mainly from devastating incidences reported in March 2011. These data were visually extracted from distinctive landslide scars found in high-resolution satellite imagery, like those from the THEOS (or Thaichote) satellite recorded on 15th April 2011 (at a spatial resolution of 2.0 m) or NASA's EO-1 satellite taken on 4th April 2011 (at a spatial resolution of 10 m). Also, distributed satellite imagery recorded over the area around that time (with landslide traces evidenced), found on the Google Earth and Bing Map websites, were also incorporated into the analysis. **Figure 3** demonstrates compared examples of several distinctive landslide scars on the used satellite imagery assembled from those 4 listed sources. Only cloud-free images were employed for this task. Eventually, a total of 210 identified landslide samples were applied for the accuracy assessment procedure of all yielded susceptibility maps.

Construction of the landslide susceptibility map

This part consists of 2 principal tasks. The first one is to formulate the landslide susceptibility maps for the area. The second task is to assess the accuracy of the resulting maps gained from each applied method. A flowchart of the main work in this part is shown in **Figure 4**. The appropriate weights of the factor and attribute (or class) level of both methods were determined from the independent judgments of 8 associated experts in this field, collected through the distributed questionnaires for each method. The net contributing weight [= Factor Weight (FW) × Class Weight (CW)], or NCW, for each attribute of a evaluated factor was then assessed (for each method) and used as a basis for the generation of the landslide susceptibility score (LSS) and the normalized susceptibility score (NSS) for a specific pixel, as follows (for 10 contributing factors);

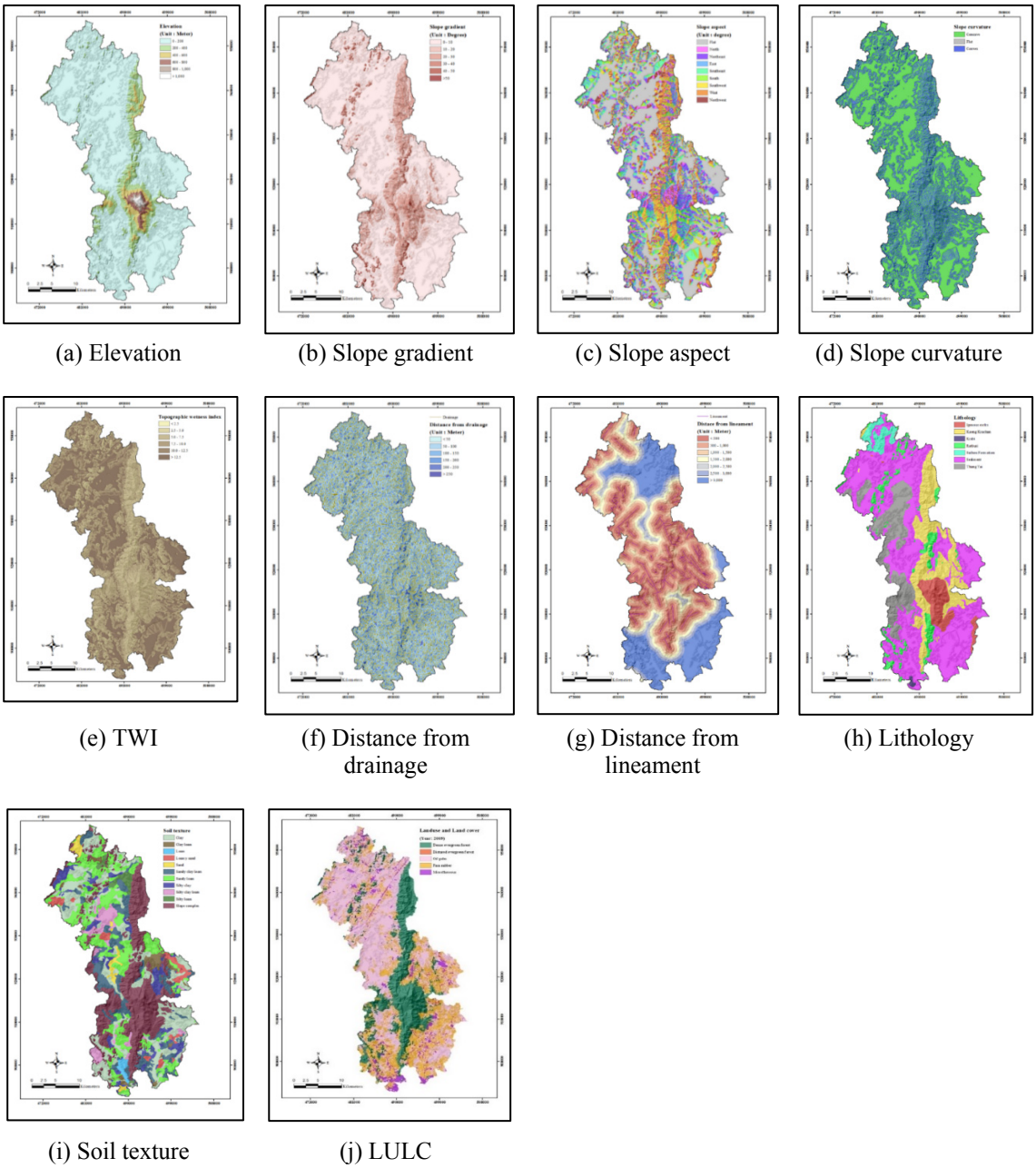

(a) Elevation (b) Slope gradient (c) Slope aspect (d) Slope curvature

(e) TWI (f) Distance from drainage (g) Distance from lineament (h) Lithology

(i) Soil texture (j) LULC

Figure 2 Landslide related factors in the study area.

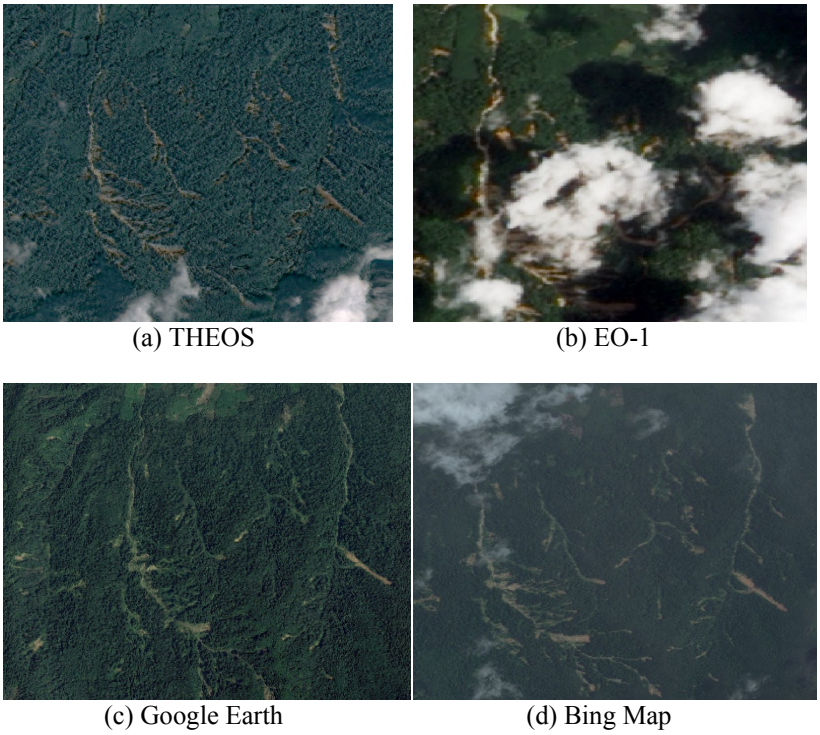

(a) THEOS (b) EO-1

(c) Google Earth (d) Bing Map

Figure 3 Examples of the high-resolution satellite images from 4 different sources; (a) THEOS satellite, (b) EO-1 satellite, (c) Google Earth website, (d) Bing Map website, showing landslide traces over the study area (from the expansive landslide incidence in late March 2011).

$$LSS_i = \sum_{j=1}^{10} NCW_{i,j} \; ; \tag{1}$$

$$NSS_i = \frac{LSS_i - LSS_{min}}{LSS_{max} - LSS_{min}}; \tag{2}$$

where LSS_i is the LSS value for pixel i^{th} on the map, and LSS_{max} and LSS_{min} are the maximum and minimum values of LSS found on the map, respectively.

NSI represents the relative probability of a landslide occurrence; therefore, the higher the index, the more susceptible the area is to landslide occurrence. If the NSI value is high, there is a higher susceptibility to landslides; a lower value indicates a lower susceptibility to landslides. These NSI values were divided into 5 classes, based on the equal interval classification method, to represent 5 different susceptibility zones on the resulting map, which are Very High Susceptibility (VHS), High Susceptibility (HS), Moderate Susceptibility (MS), Low Susceptibility (LS), and Very Low Susceptibility (VLS).

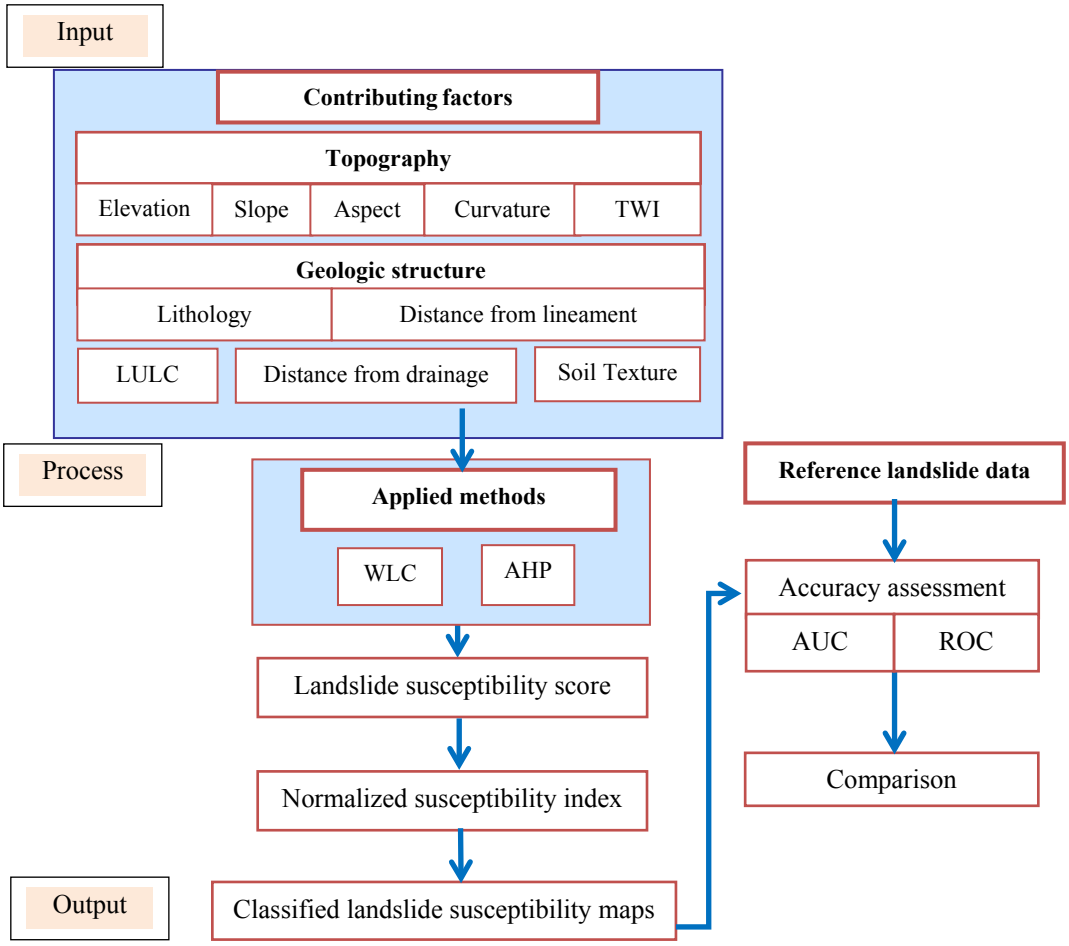

Figure 4 Work flowchart for the construction and verification of the preferred landslide susceptibility maps.

Table 2 FW and class (or attribute) weights for each input data and their attributes for the WLC method in which the proposed range of both weight types is from 1 (least important) to 5 (most important).

Thematic layers	Attributes	FW	CW	Net contributing weights (FW·CW)
Elevation	< 200 m	2.38	1.25	2.9750
	200 m – 400 m		2.13	5.0694
	400 m – 600 m		2.88	6.8544
	600 m – 800 m		3.88	9.2344
	800 m – 1,000 m		4.63	11.0194
	> 1,000 m		4.50	10.7100
Slope gradient	0º – 10º	4.50	1.00	4.5000
	10º – 20º		2.00	9.0000
	20º – 30º		3.00	13.5000
	30º – 40º		3.88	17.4600
	40º – 50º		4.13	18.5850
	> 50º		4.38	19.7100

Thematic layers	Attributes	FW	CW	Net contributing weights (FW·CW)
Slope aspect	Flat	2.38	1.00	2.3800
	North		1.50	3.5700
	Northeast		2.50	5.9500
	East		2.88	6.8544
	Southeast		2.50	5.9500
	South		3.00	7.1400
	Southwest		3.63	8.6394
	West		3.63	8.6394
	Northwest		2.25	5.3550
Slope curvature	Concave (-)	2.75	2.50	6.8750
	Flat (0)		1.38	3.7950
	Convex (+)		3.50	9.6250
TWI	0 – 2.5	2.88	1.00	2.8800
	2.5 – 5.0		2.00	5.7600
	5.0 – 7.5		3.00	8.6400
	7.5 – 10.0		3.75	10.8000
	10.0 – 12.5		4.75	13.6800
	> 12.5		5.00	14.4000
Drainage	< 50 m	2.88	4.88	14.0544
(Distance from drainage)	50 m – 100 m		4.13	11.8944
	100 m – 150 m		3.25	9.3600
	150 m – 200 m		2.25	6.4800
	200 m – 250 m		1.38	3.9744
	> 250 m		1.00	2.8800
Lithology	Thung Yai	4.29	3.14	13.4706
	Ratburi		1.57	6.7353
	Sediment		1.57	6.7353
	Kaeng Krachan		3.71	15.9159
	Igneous rocks		5.00	21.4500
	Krabi		3.00	12.8700
	Saibon Formation		3.00	12.8700
Lineament	< 500 m	3.00	5.00	15.0000
(Distance from	500 m – 1,000 m		4.13	12.3900
lineament)	1,000 m – 1,500 m		2.88	8.6400
	1,500 m – 2,000 m		2.13	6.3900
	2,000 m – 2,500 m		1.63	4.8900
	2,500 m – 3,000 m		1.25	3.7500
	> 3,000 m		1.13	3.3900
Soil Texture	Clay	3.88	1.88	7.2944
	Silty clay		2.13	8.2644
	Loamy sand		3.25	12.6100
	Sandy loam		3.13	12.1444
	Silty clay loam		3.00	11.6400
	Sand		3.25	12.6100
	Sandy clay loam		3.13	12.1444
	Clay loam		2.38	9.2344
	Silty loam		2.63	10.2044
	Loam		2.88	11.1744
	Slope complex area		3.63	14.0844
LULC	Dense evergreen forest	3.00	1.38	4.1400
	Disturbed evergreen forest		2.88	8.6400
	Oil palm		3.50	10.5000
	Para rubber		4.00	12.0000
	Miscellaneous		3.50	10.5000

Results and discussion

Weight quantification in the WLC method

From knowledge of the expert-based weighting data obtained in the WLC method (as reported in **Table 2**), it was obvious that, in terms of the priority, slope gradient, lithology, and soil texture were rated highest, with respective FW of 4.50, 4.29, and 3.88, while elevation, slope aspect, and slope curvature were scored lowest, with FW of 2.38, 2.38, and 2.75. At attribute level, the preferable conditions for landslide occurrence were high elevation (e.g. > 800 m), steep slope (e.g. > 40º), high TWI (e.g. > 10.0), relatively close distance to drainage (e.g. < 200 m) and the lineament (e.g. < 1,000 m), and igneous rock foundation. The most favorable aspects were found to be the southwest and west directions, with equal CW of 3.63. For the LULC aspect, para rubber planting was rated the most significant cause of landslide activity in the area (with CW of 4.00). The factor's order of priority (in terms of the factor weight) found in this work is rather similar to that presented in several WLC-based works reported earlier, especially on the favored top 2 candidates (slope gradient and lithology), e.g., in the works of [16,18,19]. For the attribute's merit (in terms of the attained class weight) of each of the listed factors, it often conforms well to conventional beliefs or prevalent theories. For examples, areas with higher slope gradients should be more susceptible to slope failure, as are those located closer to the drainage or lineament, or with igneous rock foundation. Areas situated in slope complex areas are also believed to most prone to landslide activity.

Weight quantification in the AHP method

The AHP method is also a very popular qualitative approach in decision-making analysis. However, in addition to the expert-based judgment on the value of the possible option, the consistency of this judgment by an individual expert is also examined. In this method, a pair-wise comparison matrix was established first from the comparative judgment of each corresponding expert, to attain a preference scale of these used factors (and the respective attributes), given in terms of a normalized weight between 0 and 1. In this case, the validity of each given judgment was determined, and those with a consistency ratio (CR) of < 0.10 were included in further analysis. **Tables 3** and **4** present the normalized weight outputs for all input factors and their respective set of attributes, while **Table 5** summarizes the yielded values of the Factor Weights and Class Weights (FW and CW) reported earlier in **Tables 3** and **4**.

Table 3 FW from pair-wise comparison matrix yielded from 8 experts.

Factors (Input layer)	FW from individual expert judgment								Mean weights (CR < 0.1)
	1	2	3	4	5	6	7	8	
Elevation	0.0227	0.0735	0.0460	0.0551	0.0206	0.0181	0.0802	0.0200	0.0550
Slope gradient	0.2796	0.2431	0.2652	0.0468	0.2601	0.2807	0.2015	0.1101	0.1733
Slope aspect	0.0600	0.0171	0.0276	0.0776	0.1790	0.0194	0.0692	0.0671	0.0517
Slope curvature	0.0297	0.1179	0.0295	0.0806	0.1292	0.0346	0.0355	0.1127	0.0752
TWI	0.0415	0.0332	0.0718	0.0692	0.0271	0.0933	0.0423	0.1807	0.0794
Drainage	0.1625	0.0170	0.0918	0.0702	0.0457	0.0626	0.0395	0.0540	0.0545
Lithology	0.1014	0.2511	0.1646	0.1663	0.1327	0.0986	0.0211	0.2750	0.1756
Lineaments	0.0675	0.1513	0.1815	0.0522	0.0413	0.0813	0.0478	0.0908	0.1047
Soil texture	0.1529	0.0588	0.1011	0.1481	0.1047	0.1498	0.2314	0.0526	0.1184
LULC	0.0820	0.0370	0.0211	0.2339	0.0595	0.1617	0.2314	0.0370	0.1121
Consistency ratio:	0.15	**0.07**	**0.09**	**0.09**	0.14	0.12	**-0.03**	**0.07**	

Note: Only judgments with CR < 0.1 were used to calculate mean weight.

From the data shown in **Table 3**, slope gradient, lithology, and soil texture are still on top in terms of preference, like in the WLC method, with FW of 0.1733, 0.1756, and 0.1184, respectively, while the 3 lowest scores now belong to aspect, drainage, and elevation, with FW of 0.0517, 0.0545, and 0.0550,

respectively. At attribute level (based on data in **Table 4**), the favorite areas for landslide activity resemble those of the WLC method, e.g., those with relatively high elevation, steep slope, close distance to the lineament and drainage system, high TWI, or with igneous rock foundation. The 2 most preferred aspect choices are still the southwest and west; for LULC, these are oil palm and para rubber planting.

Table 4 CW from pair-wise comparison matrix based on expert opinions.

Factors	CW (of each factor) from individual expert judgment								Mean weight (CR < 0.1)
	1	2	3	4	5	6	7	8	
Elevation (m)									
(1) < 200	0.0408	0.0260	0.0499	0.0469	0.0372	0.0434	0.0580	0.0268	0.0387
(2) 200 – 400	0.0633	0.0471	0.1656	0.0677	0.0478	0.0655	0.0872	0.0498	0.0724
(3) 400 – 600	0.1344	0.0886	0.1937	0.1132	0.0971	0.1024	0.1226	0.0864	0.1165
(4) 600 – 800	0.4186	0.1660	0.3159	0.1132	0.1684	0.1604	0.1677	0.1824	0.2179
(5) 800 – 1,000	0.1965	0.3362	0.1523	0.2140	0.2532	0.2488	0.2302	0.2077	0.2298
(6) > 1,000	0.1464	0.3362	0.1225	0.4449	0.3962	0.3794	0.3344	0.4469	0.3246
Consistency ratio:	**0.08**	**0.05**	**0.03**	**0.10**	**0.03**	**0.02**	0.11	**0.05**	
Slope gradient									
(1) 0º – 10º	0.0484	0.0269	0.0464	0.0458	0.0361	0.0309	0.0379	0.0301	0.0378
(2) 10º – 20º	0.0731	0.0488	0.1658	0.0712	0.0549	0.0428	0.0591	0.0567	0.0733
(3) 20º – 30º	0.1868	0.1137	0.3998	0.1018	0.0767	0.0720	0.1001	0.0707	0.1459
(4) 30º – 40º	0.3730	0.1875	0.2452	0.1636	0.1397	0.1564	0.1562	0.1323	0.1997
(5) 40º – 50º	0.1494	0.3116	0.0956	0.1636	0.2543	0.2759	0.2464	0.2503	0.2144
(6) > 50º	0.1693	0.3116	0.0472	0.4541	0.4384	0.4219	0.4003	0.4599	0.3289
Consistency ratio:	**0.06**	**0.02**	**0.04**	**0.10**	**0.06**	**0.07**	0.13	**0.05**	
Slope aspect									
(1) Flat	0.0372	0.0208	0.0271	0.0358	0.0230	0.0252	0.0340	0.0141	0.0298
(2) North	0.0432	0.0345	0.0362	0.0358	0.0317	0.0252	0.0404	0.1801	0.0386
(3) Northeast	0.2485	0.0695	0.1945	0.0674	0.0718	0.0566	0.0471	0.2047	0.1399
(4) East	0.1879	0.0336	0.0530	0.1678	0.0742	0.2243	0.0471	0.0996	0.0804
(5) Southeast	0.0849	0.0336	0.1945	0.0843	0.2001	0.1948	0.0814	0.0396	0.0986
(6) South	0.0503	0.2054	0.0530	0.1662	0.2998	0.0793	0.1263	0.1369	0.1087
(7) Southwest	0.1696	0.3730	0.1945	0.0843	0.1486	0.0564	0.2533	0.2293	0.2476
(8) West	0.1181	0.1960	0.0530	0.2523	0.0832	0.2762	0.2533	0.0727	0.1551
(9) Northwest	0.0603	0.0336	0.1945	0.1061	0.0676	0.0621	0.1172	0.0231	0.1014
Consistency ratio:	**0.07**	**0.04**	**0.04**	0.20	0.18	0.21	**0.05**	0.22	
Slope curvature									
(1) Concave (-)	0.5247	0.1749	0.2521	0.1285	0.1062	0.2605	0.4286	0.2605	0.2691
(2) Flat (0)	0.1416	0.0472	0.0726	0.2766	0.2605	0.1062	0.1429	0.1062	0.1544
(3) Convex (+)	0.3338	0.1113	0.6752	0.5949	0.6333	0.6333	0.4286	0.6333	0.4812
Consistency ratio:	**0.05**	**0.10**	0.11	**0.00**	**0.03**	**0.03**	**0.00**	**0.03**	
TWI									
(1) < 2.5	0.3915	0.0248	0.0563	0.0469	0.0408	0.3451	0.0379	0.0249	0.0387
(2) 2.5 – 5.0	0.0638	0.0435	0.4276	0.0677	0.0530	0.2093	0.0591	0.0439	0.1271
(3) 5.0 – 7.5	0.0739	0.0789	0.3305	0.1132	0.0920	0.1474	0.1001	0.0956	0.1420
(4) 7.5 – 10.0	0.1031	0.1385	0.0933	0.1132	0.1522	0.1132	0.1562	0.1574	0.1309
(5) 10.0 – 12.5	0.1502	0.2330	0.0487	0.2140	0.2475	0.1044	0.2464	0.3904	0.2267
(6) > 12.5	0.2176	0.4814	0.0436	0.4449	0.4144	0.0805	0.4003	0.2879	0.3344
Consistency ratio:	0.14	**0.10**	**0.05**	**0.10**	**0.07**	0.15	0.13	**0.10**	

Factors	CW (of each factor) from individual expert judgment								Mean weight (CR < 0.1)
	1	2	3	4	5	6	7	8	
Drainage									
Distance from drainage (m)									
(1) < 100	0.3425	0.4625	0.4996	-	0.3598	0.4467	0.0249	0.3763	0.3408
(2) 100 – 200	0.2067	0.2550	0.2944	-	0.2154	0.1893	0.0439	0.2959	0.2223
(3) 200 – 300	0.1448	0.1403	0.0872	-	0.1514	0.1408	0.0956	0.1542	0.1193
(4) 300 – 400	0.1260	0.0736	0.0409	-	0.1013	0.1033	0.1574	0.1011	0.0932
(5) 400 – 500	0.1003	0.0343	0.0389	-	0.0911	0.0728	0.3904	0.0455	0.1273
(6) > 500	0.0798	0.0343	0.0389	-	0.0810	0.0471	0.2879	0.0270	0.0970
Consistency ratio:	0.17	**0.05**	**0.06**	-	0.2	0.12	**0.10**	**0.08**	
Lithology									
(1) Thung Yai	0.1660	0.0672	0.0977	0.1075	0.2016	0.1030	-	0.1980	0.1362
(2) Ratburi	0.0328	0.0626	0.0217	0.0742	0.0685	0.0525	-	0.0540	0.0602
(3) Sediment	0.0578	0.0626	0.0219	0.0433	0.0319	0.0348	-	0.1170	0.0650
(4) Kaeng Krachan	0.1185	0.1195	0.2323	0.1228	0.0905	0.1773	-	0.0785	0.1262
(5) Igneous rocks	0.3778	0.4019	0.4135	0.2267	0.3622	0.3383	-	0.3614	0.3088
(6) Krabi	0.1309	0.2241	0.0828	0.2128	0.0959	0.1919	-	0.0217	0.1421
(7) Saibon Formation	0.1162	0.0620	0.1300	0.2128	0.1494	0.1023	-	0.1694	0.1615
Consistency ratio:	0.20	0.28	0.17	**0.02**	0.12	**0.02**	-	**0.08**	
Lineament									
Distance from lineament (m)									
(1) < 500	0.3231	0.3176	0.5302	0.1692	0.2952	0.3817	0.4007	0.3515	0.3455
(2) 500 – 1,000	0.2482	0.3176	0.1864	0.2429	0.1897	0.2486	0.1772	0.2367	0.2467
(3) 1,000 – 1,500	0.1644	0.1675	0.1100	0.2376	0.1391	0.1349	0.1371	0.1630	0.1629
(4) 1,500 – 2,000	0.1152	0.0944	0.0450	0.1776	0.1232	0.0860	0.1059	0.0933	0.1019
(5) 2,000 – 2,500	0.0614	0.0515	0.0433	0.0576	0.1012	0.0792	0.0804	0.0893	0.0637
(6) 2,500 – 3,000	0.0495	0.0257	0.0475	0.0576	0.0844	0.0441	0.0587	0.0456	0.0450
(7) > 3,000	0.0382	0.0257	0.0376	0.0576	0.0672	0.0256	0.0399	0.0206	0.0342
Consistency ratio:	**0.07**	**0.04**	**0.06**	**-0.02**	0.14	**0.02**	0.12	**0.07**	
Soil Texture									
(1) Clay	0.0224	0.0155	0.0314	0.0783	0.2734	0.1318	0.0218	0.0174	0.0494
(2) Silty clay	0.0722	0.0155	0.2020	0.0939	0.3119	0.0701	0.0332	0.0311	0.0743
(3) Loamy sand	0.1155	0.1817	0.0372	0.0511	2.8293	0.0585	0.1367	0.0873	0.0921
(4) Sandy loam	0.1341	0.1817	0.0387	0.0567	2.1233	0.0561	0.1103	0.1438	0.0979
(5) Silty clay loam	0.0514	0.0532	0.1683	0.0991	1.7464	0.1038	0.0491	0.0532	0.0878
(6) Sand	0.2871	0.1817	0.0317	0.0318	1.0172	0.0262	0.2161	0.2175	0.1175
(7) Sandy clay loam	0.1125	0.0946	0.1620	0.0991	0.8624	0.0488	0.0888	0.0356	0.0882
(8) Clay loam	0.0400	0.0155	0.0344	0.1512	0.5413	0.1252	0.0483	0.0995	0.0790
(9) Silty loam	0.0779	0.0256	0.0405	0.1512	0.4499	0.0772	0.0562	0.1624	0.0855
(10) Loam	0.0550	0.0532	0.0403	0.1512	0.4898	0.0731	0.0562	0.0831	0.0762
(11) Slope complex area	0.0317	0.1817	0.2135	0.0365	3.3229	0.2292	0.1833	0.0692	0.1522
Consistency ratio:	0.11	**0.03**	**0.04**	**-0.28**	0.14	**0.08**	**0.08**	**-0.29**	
LULC									
(1) Dense evergreen forest	0.1106	0.0299	0.3512	0.0661	0.5158	0.0494	0.0912	0.0334	0.1439
(2) Disturbed evergreen forest	0.2052	0.0855	0.1613	0.2303	0.0858	0.0806	0.1280	0.0679	0.0896
(3) Oil palm	0.2339	0.3600	0.0542	0.2910	0.2133	0.4561	0.3548	0.1748	0.3118
(4) Para rubber	0.4002	0.3600	0.1939	0.2773	0.1422	0.2616	0.3548	0.2508	0.2739
(5) Miscellaneous	0.0501	0.1646	0.2394	0.1352	0.0428	0.1523	0.0713	0.4731	0.1808
Consistency ratio:	0.11	**0.05**	0.14	0.19	**0.09**	**0.04**	**0.08**	**0.04**	

Table 5 FW and class (or attribute) weights of all input factors from the AHP method in which the possible range of both weight types is from 0 (least important) to 1 (most important).

Thematic layers	Attributes	FW	CW	FW·CW
Elevation	< 200 m	0.0550	0.0387	0.0021
	200 m – 400 m		0.0724	0.0040
	400 m – 600 m		0.1165	0.0064
	600 m – 800 m		0.2179	0.0120
	800 m – 1,000 m		0.2298	0.0126
	> 1,000 m		0.3246	0.0179
Slope gradient	0º – 10º	0.1734	0.0378	0.0066
	10º – 20º		0.0733	0.0127
	20º – 30º		0.1459	0.0253
	30º – 40º		0.1997	0.0346
	40º – 50º		0.2144	0.0372
	> 50º		0.3289	0.0570
Slope aspect	Flat	0.0517	0.0298	0.0015
	North		0.0386	0.0020
	Northeast		0.1399	0.0072
	East		0.0804	0.0042
	Southeast		0.0986	0.0051
	South		0.1087	0.0056
	Southwest		0.2746	0.0142
	West		0.1551	0.0080
	Northwest		0.1014	0.0052
Slope curvature	Concave (-)	0.0753	0.2691	0.0203
	Flat (0)		0.1544	0.0116
	Convex (+)		0.4812	0.0362
TWI	0 – 2.5	0.0794	0.0387	0.0031
	2.5 – 5.0		0.1271	0.0101
	5.0 – 7.5		0.1420	0.0113
	7.5 – 10.0		0.1309	0.0104
	10.0 – 12.5		0.2267	0.0180
	> 12.5		0.3344	0.0266
Drainage (Distance from drainage)	< 50 m	0.0545	0.3408	0.0186
	50 m – 100 m		0.2223	0.0121
	100 m – 150 m		0.1193	0.0065
	150 m – 200 m		0.0932	0.0051
	200 m – 250 m		0.1273	0.0069
	> 250 m		0.0970	0.0053
Lithology	Thung Yai	0.1756	0.1362	0.0239
	Ratburi		0.0602	0.0106
	Sediment		0.0650	0.0114
	Kaeng Krachan		0.1262	0.0222
	Igneous rocks		0.3088	0.0542
	Krabi		0.1421	0.0250
	Saibon Formation		0.1615	0.0284
Lineament (Distance from lineament)	< 500 m	0.1047	0.3455	0.0362
	500 m – 1,000 m		0.2467	0.0258
	1,000 m – 1,500 m		0.1629	0.0171
	1,500 m – 2,000 m		0.1019	0.0107
	2,000 m – 2,500 m		0.0637	0.0067
	2,500 m – 3,000 m		0.0450	0.0047
	> 3,000 m		0.0342	0.0036

Thematic layers	Attributes	FW	CW	FW·CW
Soil Texture	Clay		0.0493	0.0058
	Silty clay		0.0743	0.0088
	Loamy sand		0.0721	0.0085
	Sandy loam		0.0979	0.0116
	Silty clay loam		0.0878	0.0104
	Sand	0.1184	0.1175	0.0139
	Sandy clay loam		0.0882	0.0104
	Clay loam		0.0790	0.0094
	Silty loam		0.0855	0.0101
	Loam		0.0762	0.0090
	Slope complex area		0.1522	0.0180
LULC	Dense evergreen forest		0.1439	0.0161
	Disturbed evergreen forest		0.0896	0.0100
	Oil palm	0.1121	0.3118	0.0350
	Para rubber		0.2739	0.0307
	Miscellaneous		0.1808	0.0203

Susceptibility map construction and validation

The susceptibility map for each examined method was built from its NSS dataset, acquired through Eqs. (1) and (2) as described earlier, and the final results are illustrated in **Figures 5(a)** and **5(b)**, respectively, in which 5 susceptibility classes were identified, from VLS to VHS. In addition, the proportion of land belonging to each classified category on these maps is described conclusively in **Table 6**. From these yielded products, it was found that the 2 methods produced very similar map outlooks and distributing patterns of the classified land. Both maps conclude that most parts of the land in the study area are located in the low to very low susceptibility zone (42.86 % for the WLC and 55.85 % for the AHP), while about 17.49 % (for the WLC case) and 8.79 % (for the AHP case) of the total land area were placed in the high to very high susceptibility zone (mostly along the Khao Phanom Bencha mountain network).

The capability of these maps on the prediction of actual landslide incidence occurred was assessed using 2 popular methods: the Area-Under-Curve (AUC) analysis (as detailed in [20], and the Receiver Operating Characteristic (ROC) analysis (as detailed in [21]. Reference landslide data (of 210 samples) were taken from the landslide inventory map of the area established from original landslide evidences seen in the high-resolution satellite images, as described earlier. The primary goal of the AUC method is to quantify the accurate prediction rate of the method in use, while that for the ROC curve analysis is to find a cutoff value that shall somehow minimize the number of existing false predictions (positive or negative), or maximize the sensitivity and specificity of the prediction.

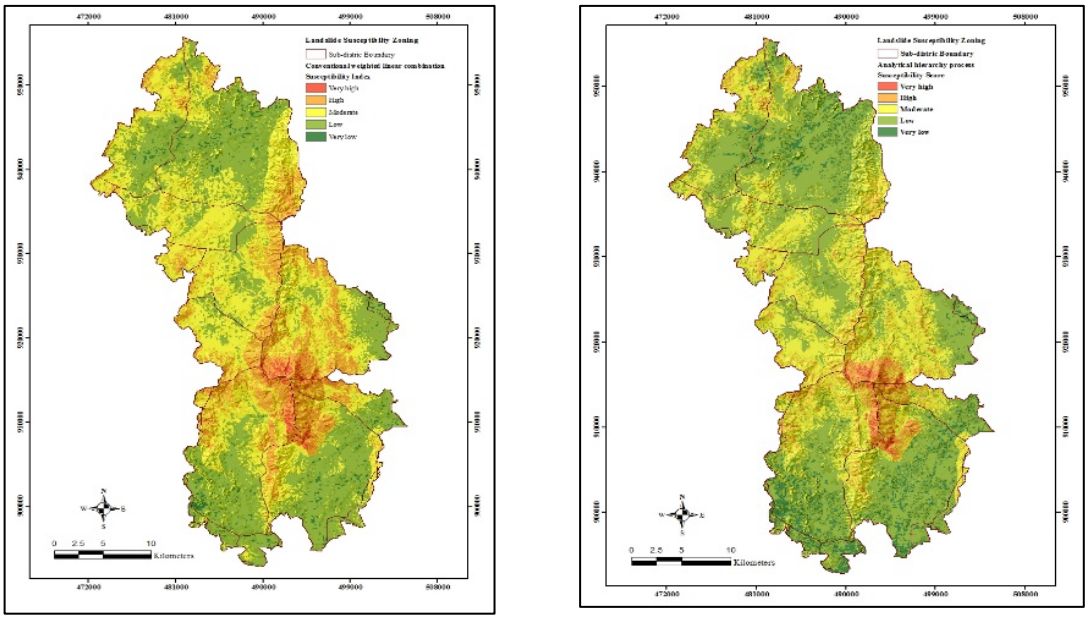

(a) WLC (b) AHP

Figure 5 The classified landslide susceptibility map based on (a) WLC and (b) AHP models.

Table 6 Landslide susceptibility classification of land for both examined methods.

Landslide susceptibility classes	NSS	Area (%)	
		WLC	AHP
VLS	0.0 - 0.2	2.11	7.37
LS	0.2 - 0.4	40.75	48.48
MS	0.4 - 0.6	39.66	35.37
HS	0.6 - 0.8	16.28	8.03
VHS	0.8 - 1.0	1.21	0.76

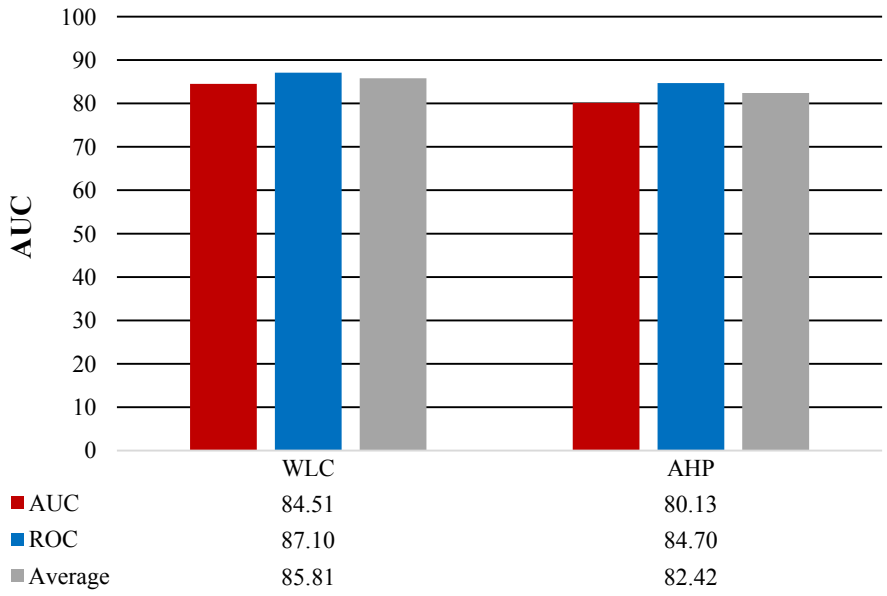

Figure 6 Achieved accuracies of the gained susceptibility maps from both examined methods (WLC/AHP).

As reported in **Figure 6**, both tested methods performed significantly well in terms of the attained accuracy, with values greater than 80 % in both the AUC and ROC cases. However, the WLC method seemed to provide a slightly better outcome than the AHP one (about 3.39 % higher in average accuracy). Therefore, the yielded susceptibility maps from both methods were fairly accurate in predicting the occurrence of past landslide incidences seen in the area and, as such, they are very useful for the formulating of landslide prone areas maps for the purposes of the prevention and mitigation of future landslide hazards within the study area. In terms of preference, the WLC method is probably more attractive than the AHP here, regarding its higher average map accuracy, as well as the rather simple concept and straightforward working process that can be fulfilled by most available GIS software nowadays.

Conclusions

This paper reports the impressive achievement of 2 preferred analysis methods, the WLC and AHP, in producing highly accurate landslide susceptibility maps for the chosen study area (Khao Phanom Bencha Watershed in Krabi Province, southern Thailand). In both cases, the appropriate weights at factor and attribute (or class) levels were evaluated first, based on the collected judgments on this issue of 8 corresponding experts, to serve as the basis for the determination of LSS and NSS afterwards. In general, the order of merit at both factor level and attribute level (in terms of the given weight), conforms rather well to conventional beliefs or prevalent theories. For example, the most important contributing factors were found to be slope gradient, lithology, and soil texture, while areas with relatively steep slopes were rated more susceptible to slope failure, as well as those located fairly close to drainage or lineament, or over the slope-complex land, or with igneous rock foundation. For the LULC aspect, para rubber and oil palm plantations were rated the most significant causes of landslide activity within the area.

The susceptibility map for each considered method was built from its NSS dataset for the whole area, wherein 5 susceptibility classes were shown, from VLS to VHS. It was found that both map products were highly similar in terms of the general outlook and the distributing pattern of the classified area, from which most lands were found located in the low to very low susceptibility zone (42.86 % for

the WLC and 55.85 % for the AHP) while a considerable amount of land was placed in the high to very high susceptibility zone (17.49 % for the WLC case and 8.79 % for the AHP case), mostly concentrated along the Khao Phanom Bencha mountain network. The average accuracies of the susceptibility maps achieved by both methods were prominently high, at 85.81 % (WLC) and 82.42 % (AHP), respectively, which ensure their applicability to further applications on landslide prevention and mitigation planning within the area. In this work, the WLC method was considered more preferable than the AHP method, regarding its superior performance in map production, along with the rather simple concept and direct working process.

Notably high accuracy of the yielded susceptibility maps in both cases indicate that the accumulated expert knowledge used in this work was fairly effective in the preparation of the landslide susceptibility map for the study area. It also highlights great concern on rather fragile geologic structure over an area, and the negative impact of the oil palm and para rubber planting on increasing potential landslide activity in the area. However, as both used methods (WLC and AHP) are of a qualitative type, whose decisions rely mainly on expert opinion, in terms of knowledge enhancement, some famous quantitative type methods, which base their judgement on actual landslide data (e.g., FR or MLR) should be applied to find the most appropriate landslide susceptibility mapping method for the area as well (apart from those reported here).

Acknowledgements

The authors are grateful to the support of the Geo-Informatics and Space Technology Development Agency (GISTDA) for providing the THEOS satellite images of the study area. Sincere thanks are also due to several state agencies for providing necessary data required in the research, including the Land Development Department, the Department of Mineral Resources, the Office of Agricultural Economics, the Royal Irrigation Department, the Royal Thai Survey Department, and the Thai Meteorological Department.

References

[1] DJ Varnes. *Landslide Hazard Zonation: A Review of Principles and Practice*. UNESCO, Paris, 1984, p. 10.
[2] DM Cruden. A simple definition of a landslide. *Bull. Int. Assoc. Eng. Geol*. 1991; **43**, 27-9.
[3] M Dilley, RS Chen, U Deichmann, AL Lerner-Lam, M Arnold, J Agwe, P Buys, O Kjekstad, B Lyon and G Yetman. *Natural Disaster Hotspots*: *A Global Risk Analysis*. World Bank, Washington DC, 2005, p. 1-17.
[4] D Petley. Global patterns of loss of life from landslides. *Geology* 2012; **40**, 939-942.
[5] B Ahmed. Landslide susceptibility mapping using multi-criteria evaluation techniques in Chittagong Metropolitan Area, Bangladesh. *Landslides* 2015; **12**, 1017-95.
[6] M Fressard, Y Thiery and O Maquaire. Which data for quantitative landslide susceptibility mapping at operational scale? Case study of the Pays d'Auge plateau hillslopes (Normandy, France). *Nat. Hazards Earth Syst. Sci*. 2014; **14**, 569-88.
[7] H Shahabi and M Hashim. Landslide susceptibility mappint using GIS-based statistical models and remote sensing data in tropical environment. *Sci. Rep.* 2015; **5**, 1-3.
[8] EA Michael and S Samanta. Landslide vulnerability mapping (LVM) using weighted linear combination (WLC) model through remote sensing and GIS techniques. *Model. Earth Syst. Environ*. 2016; **2**, 1-15.
[9] S Zhou, G Chen, L Fang and Y Nie. GIS-Based integration of subjective and objective weighting Methods for regional landslides susceptibility mapping. *Sustainability*. 2016; **8**, 1-15.
[10] I Yilmaz. Landslide susceptibility mapping using frequency ratio, logistic regression, artificial neural networks and their comparison: A case study from Kat landslides (Tokat-Turkey). *Comput. Geosci*. 2009; **35**, 1125-38.

[11] J Choi, HJ Oh, HJ Lee, C Lee and S Lee. Combining landslide susceptibility maps obtained from frequency ratio, logistic regression, and artificial neural network models using ASTER images and GIS. *Eng. Geol*. 2012; **124**, 12-23.
[12] C Xu, X Xu, F Dai and AK Saraf. Comparison of different models for susceptibility mapping of earthquake triggered landslides related with the 2008 Wenchuan earthquake in China. *Comput. Geosci*. 2012; **46**, 317-29.
[13] S Park, C Choi, B Kim and J Kim. Landslide susceptibility mapping using frequency ratio, analytic hierarchy process, logistic regression, and artificial neural network methods at the Inje area, Korea. *Environ. Earth Sci*. 2013; **68**, 1443-64.
[14] M Zare, MH Jouri, T Salarian, D Askarizadeh and S Miarrostami. Comparing of bivariate statistic, AHP and combination methods to predict the landslide hazard in northern aspect of Alborz Mt. (Iran). *Int. J. Agr. Crop Sci*. 2014; **7**, 543-54.
[15] Department of Mineral Resources. Landslide Hazard Map at Community Level for Krabi Province (*in Thai*), Available at: http://www.dmr.go.th/ewtadmin/ewt/dmr_web/images/article/freetemp/article_20110801154204.pdf, accessed December 2013.
[16] C Tanavud, C Yongchalermchai, A Bennui and C Navanugraha. Applications of GIS and remote sensing for landslide disaster management in southern Thailand. *J. Nat. Disast. Sci.* 2000; **22**, 67-74.
[17] JSM Fowze, DT Bergado, S Soralump, P Voottipreux and M Dechasakulsom. Rain-triggered landslide hazards and mitigation measures in Thailand: From research to practice. *Geotext. Geomembran.* 2012; **30**, 50-64.
[18] AN Matori, A Basith and ISH Harahap. Study of regional monsoonal effects on landslide hazard zonation in Cameron Highlands, Malaysia. *Arabian J. Geosci.* 2012; **5**, 1069-84.
[19] P Kayastha, MR Dhital and FD Smedt. Evaluation and comparison of GIS basedlandslide susceptibility mapping procedures in Kulekhani watershed, Nepal. *J. Geol. Soc. India.* 2013; **81**, 219-31.
[20] H Vijith and G Madhu. Estimating potential landslide sites of an upland sub-watershed in Western Ghat's of Kerala (India) through frequency ratio and GIS. *Environ. Geol*. 2008; **55**, 1397-405.
[21] HR Pourghasemi, C Gokceoglu, B Pradhan and KD Moezzi. *Landslide Susceptibility Mapping using a Spatial Multcriteria Evaluation Model at Hataz Watershed, Iran*. *In*: B Pradhan and M Buchroithner (eds.). Terrigenous Mass Movements. Springer-Verlag, Berlin Heidelberg, 2012, p. 23-49.